COMMUNICATIONS BIOLOGY

ARTICLE

DOI: 10.1038/s42003-018-0072-0 OPEN

A universal bioluminescence resonance energy transfer sensor design enables high-sensitivity screening of GPCR activation dynamics

Hannes Schihada[1], Sylvie Vandenabeele[1], Ulrike Zabel[1], Monika Frank[1], Martin J. Lohse[1,2] & Isabella Maiellaro[1]

G-protein-coupled receptors (GPCRs) represent one of the most important classes of drug targets. The discovery of new GCPR therapeutics would greatly benefit from the development of a generalizable high-throughput assay to directly monitor their activation or de-activation. Here we screened a variety of labels inserted into the third intracellular loop and the C-terminus of the α_{2A}-adrenergic receptor and used fluorescence (FRET) and bioluminescence resonance energy transfer (BRET) to monitor ligand-binding and activation dynamics. We then developed a universal intramolecular BRET receptor sensor design to quantify efficacy and potency of GPCR ligands in intact cells and real time. We demonstrate the transferability of the sensor design by cloning β_2-adrenergic and PTH1-receptor BRET sensors and monitored their efficacy and potency. For all biosensors, the Z factors were well above 0.5 showing the suitability of such design for microtiter plate assays. This technology will aid the identification of novel types of GPCR ligands.

[1] Institute of Pharmacology and Toxicology and Rudolf Virchow Center, University of Würzburg, Würzburg, Germany. [2] Max Delbrück Center for Molecular in Medicine, Berlin, Germany. Correspondence and requests for materials should be addressed to M.J.L. (email: lohse@toxi.uni-wuerzburg.de) or to I.M. (email: isabella.maiellaro@toxi.uni-wuerzburg.de)

G-protein-coupled receptors (GPCRs) constitute the largest and the most diverse group of membrane receptors in eukaryotes. They play a role in a plethora of cellular processes. Despite their functional diversity, they share a similar molecular architecture of seven transmembrane helices and a conserved mechanism of activation. Binding of agonist ligands to their cognate receptor leads to a change in the arrangement of distinct transmembrane helices, and a pronounced outward movement of helix 6 (up to 14 Å)[1], which is then propagated to the third intracellular loop that connects helix 5 with 6, thus enabling the engagement of several downstream signaling pathways, most importantly the activation of G-proteins. We previously demonstrated that such ligand-induced conformational changes can be visualized in living cells by Förster Resonance Energy Transfer (FRET). The average distance between the third intracellular loop and the C-terminus of receptors (e.g., β_2AR 6.2 nm)[2] is within the range addressable by FRET (2.4–7.2 nm)[3]. Therefore, tagging these conformationally sensitive sites with fluorescent donors and acceptors permits the recording of receptor activation as a change in energy transfer between these chromophores. Following this principle, a series of intramolecular FRET-based GPCR-biosensors have been generated, notably for the α_{2A}-adrenergic receptor (α_{2A}AR), employing the fluorescent proteins CFP and YFP ($\alpha_{2A}AR_{CFP/YFP}$)[4,5] or CFP with the small Fluorescein Arsenical Hairpin Binder (FlAsH) as fluorophores[6].

These FRET-based GPCR biosensors have become widely used tools[7] and represent the most direct unbiased way to determine the effects of ligands on a given receptor. Their employment has helped to elucidate several aspects of receptor pharmacology and kinetics[8]. However, the combination of donor and acceptor fluorophores used so far suffers from a low signal-to-noise ratio and high fluorescence background which limits their use to single-cell experiments, slowing down the characterization of new pharmacological compounds as GPCR-directed therapeutics. More recently, Bioluminescence Resonance Energy Transfer (BRET) has been tested as an alternative approach to monitor the conformational change of receptors. BRET occurs between proximally situated donor–acceptor pairs (1.6–8.5 nm)[9], but here a light emitting enzyme luciferase is used as a donor, sidestepping many of the deficiencies associated with direct illumination of the sample. Earlier attempts to generate intramolecular GPCR BRET-based biosensors employing Renilla Luciferase as a donor in combination with GFP or FlAsH as acceptor showed poor agonist-induced BRET changes[10–13].

Despite the many efforts in optimizing the way in which we study GPCRs and a plethora of methods to assess ligand binding or downstream signaling, the lack of a generalizable assay to monitor directly in living cells receptor activation or de-activation in a format suitable for high-throughput screening is slowing down the progress in discovering new GPCR therapeutics. In the present study, we therefore set out to permutate the well-characterized FRET-based biosensor $\alpha_{2A}AR_{CFP/YFP}$ in order to develop a universal and versatile sensor design to reach the stringent requirements of monitoring receptor conformational dynamics in intact cells in microtiter plates.

Preserving the fluorophore insertion sites in the third intracellular loop and C- terminus, we investigated whether combining different donors and acceptors would improve the transfer of energy to enable the visualization of the receptor's conformational changes in microtiter plates. Among the 10 FRET-based and the 11 BRET-based α_{2A}AR biosensors generated in this study, the highest amplitude in the signals upon norepinephrine stimulation was recorded with the BRET-based α_{2A}AR biosensors combining NanoLuc[14] luciferase as the donor and the self-labeling protein tag Halo labeled with the HaloTag dye NanoBRET 618 as the acceptor. The EC_{50}-values calculated for these BRET experiments were in line with binding affinities, demonstrating that the developed BRET biosensor $\alpha_{2A}AR_{Nluc/Halo}$ assay faithfully reports ligand affinities. This feature was conserved also for a β_2-adrenergic and a PTH1 receptor BRET-based biosensors. Also for these two receptors, the agonist-induced BRET changes were in line with the binding data suggesting that our receptor biosensor design is a generalizable design that may be use in lieu of the endogenous receptor to determine efficacy and potency of ligands. To assess the applicability of the biosensor design to microtiter plate and its scalability, we performed for each receptor a Z-factor analysis[15] to quantify the quality and reproducibility of the assays. For all receptors analyzed, the Z-factor was well above 0.5—which characterizes an excellent assay suitable to be used in microtiter plates. We propose that this technology will speed the characterization of new pharmacological compounds acting at GPCRs.

Results

Dynamic range of FRET- and BRET-based α_{2A}AR biosensors. With the goal of generating a GPCR biosensor design to monitor receptor activation in microtiter plates, we permutated the well-characterized FRET-based biosensor $\alpha_{2A}AR_{CFP/YFP}$. We preserved the fluorophore insertion sites in the third intracellular loop and C-terminus (Fig. 1a) but we substituted the original YFP with its brighter variant cpVenus or with self-labeling protein tags: *SNAP* ($\alpha_{2A}AR_{CFP/SNAP}$; 20 kDa)[16] or *Halo* ($\alpha_{2A}AR_{CFP/Halo}$; 36 kDa)[17]. Both of these tags can be labeled covalently with exogenous cell-permeable fluorescent dyes. Their diverse emission and excitation peaks (Fig. 1b, Supplementary Fig. 1), degrees of spectral overlap with the donor emission (CFP) and photophysical properties impacted the FRET behavior that we observed, allowing us to optimize our approach using a modular fluorophore within the receptor chassis. In this optimization phase, HEK cells were transiently transfected with the different α_{2A}AR biosensors and, after specific labeling, experiments were performed in 96-well plates (Fig. 1c). Each FRET-based pair exhibited a different degree of basal transfer of energy—as demonstrated by their respective FRET emission spectra (Fig. 1d). However, only five of the ten FRET-based pairs tested showed a detectable agonist-induced change in FRET (ΔFRET%) that did not exceed 5% when stimulated by the full agonist norepinephrine (100 µM) (Fig. 1e).

With the goal of obtaining a higher dynamic range, we tested BRET as possibly more sensitive approach. Here, we used the relatively small-sized NanoLuc[14] luciferase (19 kDa; Nluc) that possesses, in presence of its substrate (furimazine), a narrow bioluminescence spectrum, high brightness, and physical stability.

We generated 11 BRET-based α_{2A}AR biosensors combining the donor Nluc with fluorescent proteins of different color from yellow (cpVenus) to orange-red (mCherry; TagRFP), or with the self-labeling Halo or SNAP tags. Applying the workflow developed above (Fig. 1c), we tested the ability of the α_{2A}AR BRET biosensors to report effects of the full agonist norepinephrine in microtiter plate format. All the tested receptor BRET-sensors exhibited a basal energy transfer (Fig. 1f), while the activation of the receptor induced by norepinephrine at a concentration of 100 µM was detectable in seven of them. The highest amplitude was recorded for Nluc combined with the HaloTag dye NanoBRET 618[18] (α_{2A}-$AR_{Nluc/Halo\mathbf{618}}$; ΔBRET % = 8.15 ± 0.72) (Fig. 1g)—about two-fold higher than all other 20 FRET- and BRET-biosensors tested. No further improvement in the amplitude of ΔBRET was obtained by swapping the positions of donor and acceptor (Supplementary Fig. 2).

Pharmacology of the α_{2A}-$AR_{Nluc/Halo\mathbf{618}}$ BRET-based biosensor. We then sought to ascertain that the $\alpha_{2A}AR_{Nluc/Halo\mathbf{618}}$ faithfully recorded efficacies and potencies of a panel of known α_{2A}AR

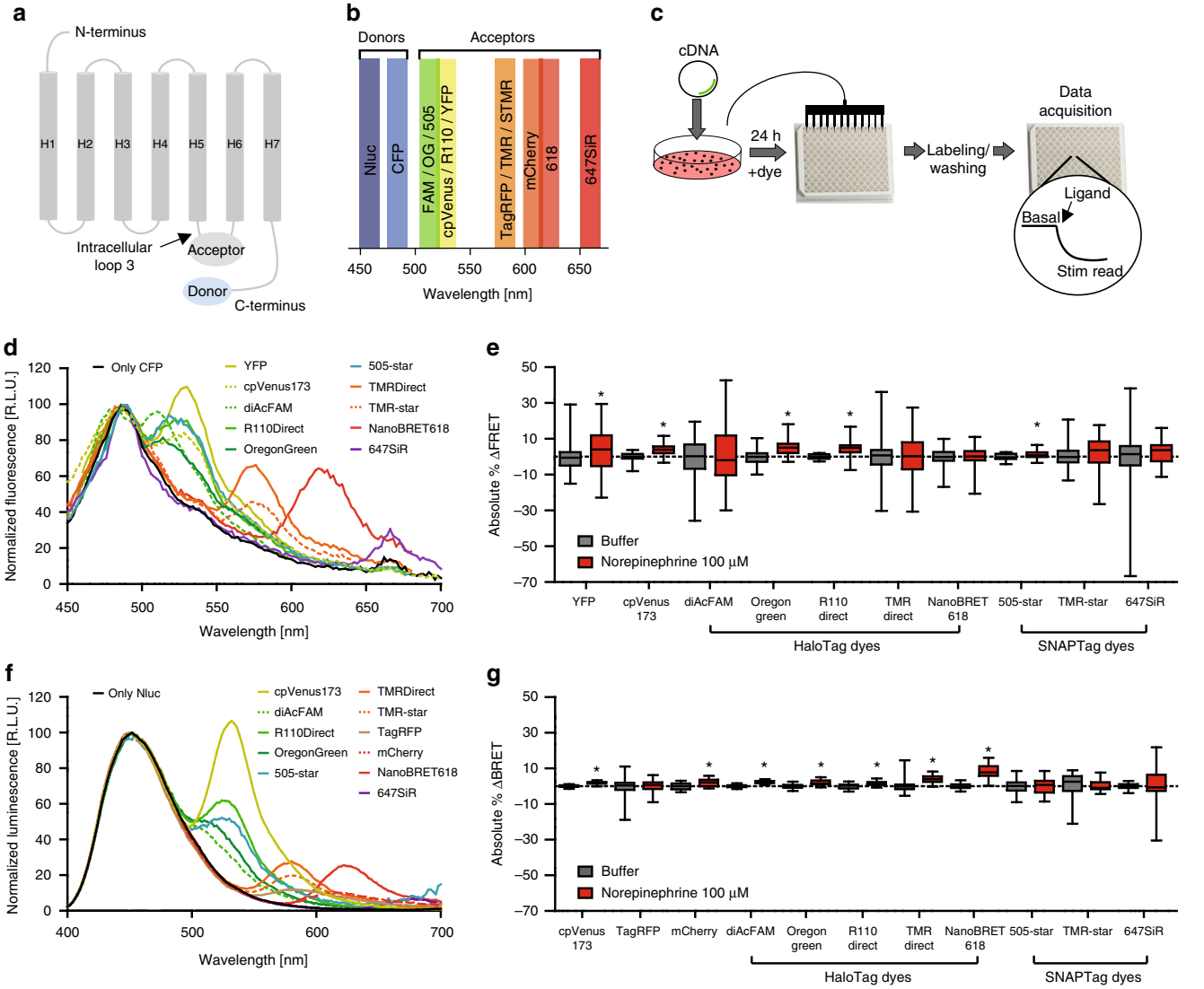

Fig. 1 Evaluation of intramolecular FRET and BRET α_{2A}-adrenergic receptor biosensors. **a** Schematic of the biosensor. **b** Emission peaks of chromophores. **c** Workflow. **d** FRET emission spectra of the CFP-label alone or with fluorescent acceptors (each $N = 1$). **e** FRET changes (%) induced by norepinephrine normalized for buffer (YFP: $N = 7$, cpVenus173: $N = 4$, diAcFAM: $N = 6$, Oregon Green: $N = 5$, R110 Direct: $N = 3$,TMR Direct: $N = 6$, NanoBRET 618: $N = 6$, 505-star: $N = 5$, TMR-star: $N = 5$, 647SiR: $N = 4$). **f** BRET emission spectra of the NanoLuc-label alone or with fluorescent acceptors (each $N = 1$). **g** BRET changes (%) induced by norepinephrine normalized for buffer (cpVenus173: $N = 7$, TagRFP: $N = 4$, mCherry: $N = 4$, diAcFAM: $N = 3$, Oregon Green: $N = 3$, R110 Direct: $N = 3$, TMR Direct: $N = 3$, NanoBRET 618: $N = 7$, 505-star: $N = 3$, TMR-star: $N = 5$, 647SiR: $N = 5$). Data in **e** and **g** show box and whisker plots. Difference was analyzed by two-way ANOVA followed by Bonferroni post hoc test. $^*p \leq 0.05$ vs. buffer

ligands (Supplementary Table 1). We created a cell line stably expressing this biosensor, and after optimizing the assay conditions (Supplementary Fig. 3), we measured ligand-induced BRET-responses. Stimulation with the full agonist norepinephrine (100 µM) and the inverse agonist yohimbine (100 µM) induced changes in BRET with opposite directions (Fig. 2a; agonist: positive ΔBRET blue line; inverse agonist: negative ΔBRET black line)—mirroring the opposite pharmacological effect exerted at the receptor level. The changes in BRET evoked by both ligands were fast, reaching a plateau 120 s after their injection, and remained stable for more than 30 min (Supplementary Fig. 4). The injection of the antagonist phentolamine (1 µM) reverted the effect of norepinephrine (Fig. 2a; red line), demonstrating the applicability of the biosensor to monitor inactivation kinetics. A panel of seven additional ligands triggered responses ranging between the two extremes, norepinephrine and yohimbine, and compatible with their known efficacies as full, partial, or inverse agonists (Fig. 2b, Supplementary Table 1). Full concentration–response curves were performed for all ten compounds (Fig. 2c). Radioligand binding experiments demonstrated that the BRET biosensor $\alpha_{2A}AR_{Nluc/Halo}$ had binding affinities (pK_i-values) similar to the wild-type receptor (Supplementary Table 2), and they correlate with the measured EC_{50}-values (Supplementary Table 3), indicating that our assay faithfully reports ligand affinities. Interestingly, for agonists these EC_{50}-values were similar to the high-affinity component of the competition curves (pK_H) generally assumed to represent the receptor/G-protein complex[19]. This indicates some constitutive activity of the $\alpha_{2A}AR_{Nluc/Halo}$ biosensor and its interaction with endogenous G-proteins. The relative BRET-change induced by neutral ligands and also the characterization of G-protein activation (Supplementary Fig. 5) demonstrated some constitutive activity of the biosensor. Such constitutive activity, not seen with analogous GFP-based sensors[20], might be due to the larger size of the tags

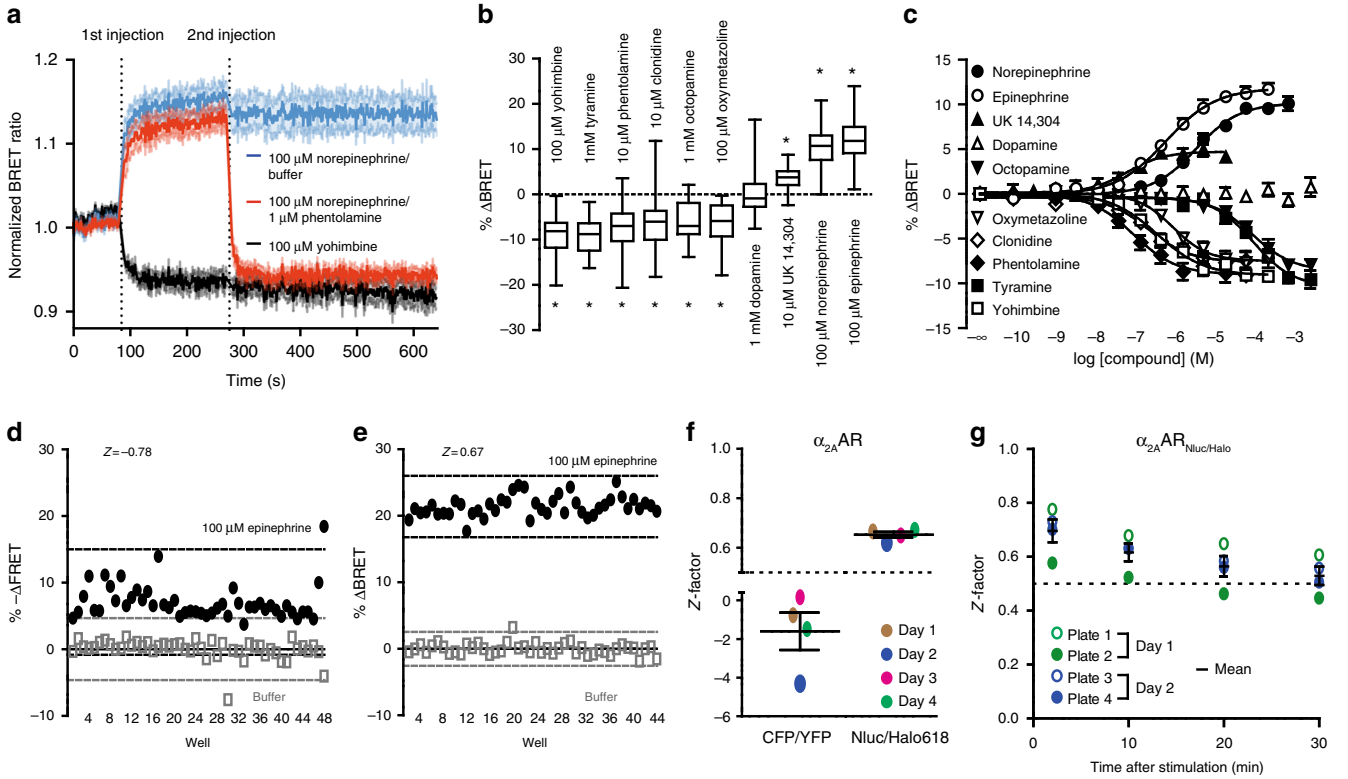

Fig. 2 Pharmacological characterization of the $\alpha_{2A}AR_{Nluc/Halo618}$ BRET-based biosensor, and evaluation of its applicability for microtiter plate screening. **a** Time-course of the normalized BRET ratio upon ligand stimulation (each $N = 3$). **b** Ligand-induced maximal BRET changes (Yohimbine: $N = 7$, Tyramine: $N = 10$, Phentolamine: $N = 11$, Clonidine: $N = 10$, Octopmaine: $N = 5$, Oxymetazoline: $N = 6$, Dopamine: $N = 6$, UK 14,304: $N = 10$, Norepinephrine: $N = 25$, Epinephrine: $N = 23$). **c** Concentration-response curves of different $\alpha_{2A}AR$ ligands (Yohimbine: $N = 7$, Tyramine: $N = 4$, Phentolamine: $N = 5$, Clonidine: $N = 4$, Oxymetazoline: $N = 4$, Octopamine: $N = 4$, Dopamine: $N = 4$, UK 14,304: $N = 3$, Norepinephrine: $N = 6$,Epinephrine: $N = 4$). Comparison of the Z-factors for cells expressing the $FRET_{CFP/YFP}$ or $BRET_{Nluc/Halo}$ sensor of $\alpha_{2A}AR$. **d** FRET or **e** BRET changes 2 min after 100 µM epinephrine or buffer stimulation are plotted for each well of representative plates and **f** the average values (each $N = 4$). **g** Z-factor at different time points after addition of 100 µM epinephrine or buffer ($N = 4$). Data show box and whisker plots (**b**) or mean ± s.e.m (**a**, **c**, **f**, **g**). Difference was analyzed by two-way ANOVA followed by Bonferroni post hoc test. $^*p \leq 0.05$ vs. buffer

employed that might separate helices 5 and 6, which would shift the receptor to a more active state. However, this effect did not change the expected order of efficacies of the various ligands and even facilitated the characterization of both, inverse agonists and antagonists. Overall, these data indicate that the intramolecular $\alpha_{2A}AR_{Nluc/Halo\mathbf{618}}$ BRET-biosensor faithfully reports the activation state of the $\alpha_{2A}AR$ in 96-well plates.

Microtiter plate suitability of the $\alpha_{2A}AR_{Nluc/Halo618}$. To validate the suitability of the novel BRET-based biosensor $\alpha_{2A}AR_{Nluc/Halo\mathbf{618}}$ to monitor receptor conformation in microtiter plate format, we performed the Z-factor analysis[15] to quantify the quality and reproducibility of the assay. In this analysis, values $Z < 0$ defines unusable assays, $Z = 1$ approximates a "perfect" assay, and $Z \geq 0.5$ characterizes an excellent assay. Compared to the original $\alpha_{2A}AR_{CFP/YFP}$, classified as unusable ($Z = -1.60 \pm 0.97$; Fig. 2d, f), $\alpha_{2A}AR_{Nluc/Halo\mathbf{618}}$ yielded an excellent assay ($Z = 0.65 \pm 0.01$; Fig. 2e, f) that was stable for more than 20 min (Fig. 2g).

β_2-adrenergic receptor BRET-biosensor ($\beta_2AR_{Nluc/Halo\mathbf{618}}$). To demonstrate the transferability of the $BRET_{Nluc/Halo\mathbf{618}}$ as a general design to pharmacologically profile any GPCR, we generated an analogous β_2-adrenergic receptor biosensor ($\beta_2AR_{Nluc/Halo\mathbf{618}}$) and measured efficacy and potency of different ligands in microtiter plate format. The $\beta_2AR_{Nluc/Halo\mathbf{618}}$ biosensor showed signaling activity similar to the wild-type receptor (Supplementary Fig. 6a–c). Full agonist stimulation induced a change in BRET opposite to that of an inverse agonist, while the amplitudes for antagonists and partial agonists were intermediate (Fig. 3a), demonstrating that the ability of reporting the efficacy of ligands was preserved. The EC_{50}-values obtained from concentration–response curves for the full agonist epinephrine, the inverse agonist ICI 118,551 and the neutral antagonist carvedilol (Fig. 3b), were similar to data obtained by radioligand binding assay (Supplementary Table 4), demonstrating the β_2AR BRET-based biosensor was reporting wild-type affinity and efficacy. Interestingly, we found that norepinephrine, usually considered a full agonist when monitored at the second messenger level[21] (cAMP), induced only a partial conformational change of $\beta_2AR_{Nluc/Halo\mathbf{618}}$—in line with other conformational studies[22,23]. Our data would also support the new evidence suggesting that UK 14,304 behaves as a partial[24] more than a full agonist. This demonstrates that BRET-based biosensors are a powerful unbiased approach, since they bypass the effect of signal amplification and receptor reserve. Again, the Z-factor of ≈ 0.8 was greatly improved compared to the earlier FRET β_2AR-biosensor and indicated the suitability for high-throughput screening (Fig. 3c; Supplementary Fig. 8)

Parathyroid hormone receptor 1 BRET-biosensor ($PTHR1_{Nluc/Halo\mathbf{618}}$). To further substantiate the transferability of the $BRET_{Nluc/Halo\mathbf{618}}$ sensor design, we devised an analogous class B parathyroid hormone receptor 1 (PTHR1) BRET-biosensor ($PTHR1_{Nluc/Halo\mathbf{618}}$). Again, this biosensor retained

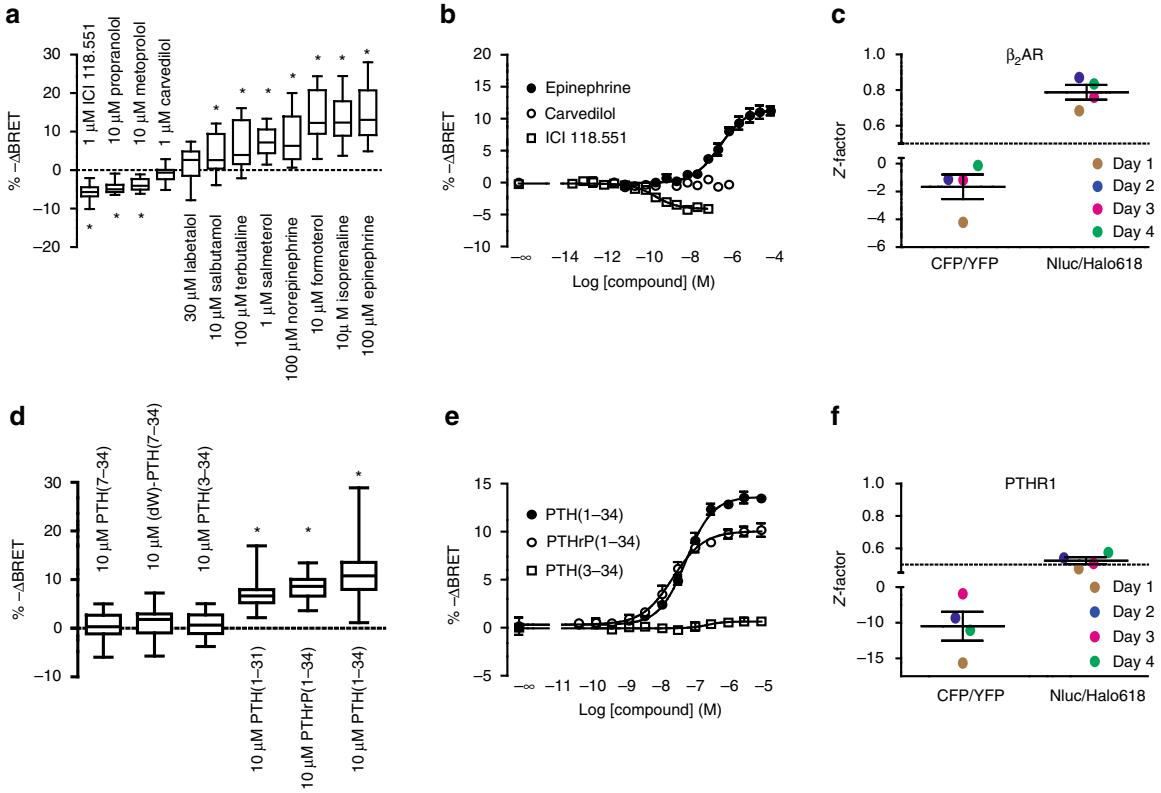

Fig. 3 Transferability and microtiter plate applicability of the new intramolecular receptor-biosensor design. BRET changes reported by $\beta_2AR_{Nluc/Halo618}$ expressing cells upon (**a**) saturating ligand stimulation (ICI 118.551: $N = 6$, Propranolol: $N = 6$, Metoprolol: $N = 6$, Carvedilol: $N = 12$, Labetalol: $N = 16$, Salbutamol: $N = 8$, Terbutaline: $N = 8$, Salmeterol: $N = 11$, Norepinephrine: $N = 8$, Formoterol: $N = 11$, Isoprenaline: $N = 21$, Epinephrine: $N = 21$) and **b** serial ligand dilutions to obtain concentration–response curves (Epnephrine: $N = 4$, Carvedilol: $N = 4$, ICI 118.551: $N = 6$). **c** Mean of the *Z*-factor of $\beta_2AR_{CFP/YFP}$ and $\beta_2AR_{Nluc/Halo618}$ (each $N = 4$). BRET changes reported by $PTHR1_{Nluc/Halo618}$ expressing cells upon (**d**) saturating ligand stimulation (PTH(7-34): $N = 12$, (dW)-PTH(7-34): $N = 12$, PTH(3-34): $N = 14$, PTH(1-31): $N = 6$, PTHrP(1-34): $N = 14$,PTH(1-34): $N = 22$) and **e** serial ligand dilutions to obtain concentration–response curves (PTH(1-34): $N = 3$, PTHrP(1-34): $N = 3$, PTH(3-34): $N = 6$). **f** Mean of the *Z*-factor of $PTHR1_{CFP/YFP}$ and $PTHR1_{Nluc/Halo618}$ (each $N = 4$). Data are expressed as box and whisker plots (**a**, **d**) or mean ± s.e.m (**b**, **c**, **e**, **f**). Difference was analyzed by two-way ANOVA followed by Bonferroni post hoc test. $^*p \leq 0.05$ vs. buffer

signaling activity (Supplementary Fig. 6d–f), efficacy (Fig. 3d) and affinity (Fig. 3e) similar to the wild-type receptors (Supplementary Table 5) for the analyzed peptides.

Application of the full agonist PTH(1-34) evoked a ≈10% change in BRET. Antagonists had no detectable effects (Fig. 3d), but retained their ability of inhibiting receptor activation in competition experiments (Supplementary Fig. 7). In contrast to the $\alpha_{2A}AR$ and β_2AR, no inverse agonists are available for the PTHR1 that might cause effects opposite to those of PTH(1-34). The *Z*-factor for $PTHR1_{Nluc/Halo618}$ (0.52 ± 0.02) demonstrated that also this BRET-biosensor was suitable for high-throughput screening (Fig. 3f; Supplementary Fig. 8).

Discussion

Taken together, we have developed a universal sensor design for GPCRs that retains the signaling capacity of the receptors, resolves both efficacy and potency of ligands, and works in intact cells and in real time in a microtiter plate format. In a single assay, this approach offers the analysis of activation/de-activation kinetics, potency and direct efficacy–which makes it a rapid and high content screening approach. The throughput of this assay essentially depends on the equipment available for pipetting and plate reading. Under optimal conditions, it depends only on the time required to read the plate before and after addition of compounds, while under the most basic conditions, the time required for a single plate would encompass the times required for the basal read, addition of compounds, and a second read. If the labeling procedure is carried out in serum- and phenol red-free medium, then no washing step is required.

As any optical detection method, the readout of our BRET-based receptor biosensor may be impaired by molecules that interfere with the absorption properties; bind to the energy donor or acceptor interfering with their emission properties; and compete with the substrate, causing inhibition of the luciferase[25]. The chemical evaluation of compounds of a screening library can help discriminating false positives. Appropriate controls for these issues therefore need to be included in such a screening approach. An advantage of our receptor biosensor is that the tags are localized intracellularly, which limits their susceptibility to cell permeable compounds.

To the best of our knowledge, this generalizable design offers the first possibility to upscale the study of receptor activation and deactivation - which represents the most direct and unbiased way to estimate the effect of any chemical entity on receptors of interest, facilitating the discovery of new therapeutic compounds. These GPCR biosensors should prove useful in determining ligand properties at known GPCRs and in elucidating the binding properties of orphan receptors. Furthermore, their high sensitivity may allow their use to monitor GPCR activation in situ using new knock-in technologies[26].

Methods

cDNA constructs. The FRET sensor $\alpha_{2A}AR_{CFP/YFP}$[4] was used as starting construct to generate the various α_{2A}-adrenergic receptor FRET and BRET sensors ($\alpha_{2A}AR_{donor/acceptor}$) described in this study. The donors (CFP or Nluc) were fused to Val461 at the C-terminus while all acceptors tested were placed in the third intracellular loop between Ala250 and Ser371. The BRET-based β_2-adrenergic receptor biosensor $\beta_2AR_{Nluc/Halo}$ was cloned starting from the previously described FRET version[22] introducing HaloTag in the third intracellular loop between Asp251 and Gly252 and Nluc in the C-terminus at Glu369. The BRET sensor for the parathyroid hormone receptor (PTHR1) was cloned starting from the previously described FRET version[4]. HaloTag was inserted in the third intracellular loop between Gly395 and Arg396 and Nluc was fused to Gly497 of the C terminus. All tag exchanges were performed employing established PCR strategies and restriction and ligation enzymes. Constructs were cloned into a pcDNA3 vector and verified by sequencing.

Plasmids. cDNA encoding the fluorescent protein cpVenus[173] was amplified from the $G\alpha_{i2}$-sensor v2.0[27]. The SNAPtag sequence was amplified using a SNAPtag-$GABA_{B1}$ template kindly provided by J.P. Pin (Institut de Génomique Fonctionnelle, Montpellier, France)[28]. Sequences encoding TagRFP (pTagRFP-C vector) and mCherry were purchased from Evrogen and Addgene, respectively. cDNA encoding HaloTag (pFC14K HaloTag® CMV Flexi® Vector) and NanoLuciferase (pFC32K Nluc CMV-neo Flexi® Vector) were purchased from Promega. $G\alpha_{i2}$-FRET[27] sensor was kindly provided by J. Goedhart (Section Molecular Cytology, University of Amsterdam, Amsterdam, The Netherlands), the H187-EPAC-FRET sensor[29] was kindly provided by K. Jalink (The Netherlands Cancer Institute, Amsterdam, The Netherlands).

Reagents. (−)-Epinephrine, L-(−)-norepinephrine (+)-bitartrate salt monohydrate, UK 14,304, dopamine hydrochloride, (±)-octopamine hydrochloride, clonidine hydrochloride, tyramine hydrochloride, phentolamine hydrochloride, yohimbine hydrochloride, isoprenaline hydrochloride, formoterol fumarate dihydrate, terbutaline hemisulfate salt, salmeterol xinofoate, salbutamol hemisulfate salt, metoprolol tartrate, (±)-propranolol hydrochloride, ICI 118,551 hydrochloride, labetalol hydrochloride, carvedilol, GTP, poly-D-lysine, G-418 and the fluorescent monoclonal antibody Anti-Flag® M2-Cy3 and Millipore glass-fiber filters for radioligand saturation binding were from Sigma-Aldrich. [^{3}H]RX821002 was purchased from Hartmann Analytic. The HA-tag monoclonal antibody (16B12) Alexa Fluor 488 was from ThermoFisher Scientific. Oxymetazoline hydrochloride was purchased from Tocris. The peptide ligands PTH(1-34) (catalog number: H-4835), PTH(7-34) (catalog number: N-1110), (dw)-PTH(7-34) (catalog number: H-9115), PTHrP(1-34) (H-6630), PTH(1-31) (catalog number: H-3408) and PTH(3-34) (catalog number: H-3088) were from BACHEM. All HaloTag fluorescent dyes were purchased from Promega. SNAP fluorescent dyes were from NEB. White-wall, white bottomed and black-wall, black-bottomed 96-well plates were purchased from Brand. MultiScreen® Filter plates for radioligand competition binding were from Millipore.

Cell culture and transfection. HEK-TSA cells used for transient expression of constructs, were grown in Dulbecco's Modified Eagle's Medium (DMEM) supplemented with 2 mM glutamine, 10% fetal calf serum, 0.1 mg mL^{-1} streptomycin, and 100 units per mL penicillin at 37 °C with 5% CO_2. HEK293 cells were used for the development of stable BRET sensor cell lines. Cells grown in 100 mm dishes were transfected at a confluence of 50–70% with 5 µg of DNA using Effectene Transfection Reagent Kit (Qiagen) according to the manufacturer's instructions. Transfected clones were selected with 600 µg mL^{-1} of G-418 and clonal lines were maintained in DMEM supplemented with 200 µg mL^{-1} G-418, 2 mM glutamine, 10% fetal calf serum, 0.1 mg mL^{-1} streptomycin, and 100 units per mL penicillin at 37 °C with 5% CO_2.

Transient transfection and plating. For transient expression of the sensors, 1.5×10^6 HEK-TSA cells were seeded onto a 55 mm dish and transfected the day after with 2 µg of plasmids encoding the biosensors using Effectene Transfection Reagent (Qiagen) according to the manufacturer's protocol. In case two different plasmids were co-transfected, 4 µg was used as total amount of DNA in a 1:1 ratio of the two plasmids. Twenty-four hours after transfection, cells were transferred to poly-D-lysine pre-coated black-wall, black-bottomed (FRET experiments) or white-wall, white-bottomed (BRET experiments) 96-well plates at a density of 50,000 (FRET) or 20,000 (BRET) cells per well.

Fluorescence labeling of FRET and BRET acceptors. Labeling with all dyes was performed at 37 °C and 5% CO_2 in 96-well plates. All dyes were dissolved in DMEM. HaloTag® diAcFAM (1 µM), HaloTag® Oregon Green® (1 µM), SNAP-cell 505-Star (10 µM), SNAP-cell TMR-Star (3 µM) and SNAP-cell 647SiR (3 µM) were incubated for 30 min 48 h after transfections. Excessive dye was washed out three times followed by incubation with fresh DMEM for additional 30 min (37 °C and 5% CO_2). HaloTag® R110Direct, HaloTag® TMRDirect and HaloTag® NanoBRET 618 required overnight labeling at a concentration of 100 nM. A minimum of 4 wells remained unlabeled to serve as correction for donor bleedthrough (unlabeled control).

Measurement of fluorescence excitation and emission spectra. HEK-TSA cells were transfected with different BRET based α_{2A}AR biosensors and labeled as described above, without substrate, in order to read only the emission and excitation spectra of the different acceptors. YFP and CFP spectra were collected using the FRET $\alpha_{2A}AR_{CFP/Halo}$ and $\alpha_{2A}AR_{YFP/Halo}$ biosensors without HaloTag labeling. All spectra were measured in buffer (2 mM HEPES, 28 mM NaCl, 1.08 mM KCl, 0.2 mM $MgCl_2$, 0.4 mM $CaCl_2$, pH 7.3) with 2 nm resolution from 400 to 700 nm using a CLARIOstar plate reader (BMG). Spectra are expressed as a percentage of the respective maximal excitation or emission peak.

Measurement of FRET and BRET emission spectra. HEK-TSA cells were transfected and labeled as described above. Emission spectra were recorded in buffer with 2 nm resolution from 400 to 700 nm upon donor excitation at 420 nm (FRET sensors) or addition of 1:1000 furimazine dilution (BRET) using a CLARIOstar plate reader (BMG). Spectra are expressed as a percentage of the maximal donor emission peak.

FRET measurements. Cells expressing the FRET sensors were washed to substitute the DMEM with the experimental buffer. Basal FRET ratio was measured in 90 µL buffer. Subsequently, 10 µL of 10-fold ligand solution or buffer (negative control) was applied to each well and the stimulated FRET ratio was recorded. All FRET experiments were conducted at 37 °C with a Synergy Neo2 plate reader (BioTEK) equipped with 420/50 nm excitation and 485/20 nm emission filters for CFP. Acceptor emission of YFP, HaloTag® R110, HaloTag® diAcFAM, HaloTag® Oregon Green® and SNAP-cell 505-Star were detected with a 540/25 nm (FRET) filter. To measure the emission of HaloTag® TMR-Direct and SNAP-cell TMR-Star a 590/35 nm filter was used. Emission of HaloTag® NanoBRET 618 and SNAP-cell 647SiR were detected with a 620/15 nm and 680/20 nm filter, respectively. Fifty excitation flashes were applied per data point.

BRET measurements. Cells transiently or stably expressing the BRET-biosensors were washed to substitute DMEM with the experimental buffer and incubated with substrate (90 µL of 1:1000 for $\beta_2AR_{Nluc/Halo618}$ and $PTHR1_{Nluc/Halo618}$; 1:4000 for $\alpha_{2A}AR_{Nluc/Halo618}$) for 2–5 min at 37 °C to allow for substrate diffusion and the basal BRET ratio was measured. Following this, 10 µL of 10-fold ligand solution or buffer was applied to each well and the stimulated BRET ratio was recorded. To reduce the fluctuation of the BRET ratio in *Z*-factor experiments, seven individual BRET ratios within 5 min were measured and averaged before and after ligand addition.

BRET experiments were performed at 37 °C with a GloMAX Discover (Promega) or Synergy Neo2 (BioTEK) plate reader equipped with a 460/40 nm filter to select the NanoLuc emission. For cpVenus173, HaloTag® R110, HaloTag® diAcFAM, HaloTag® Oregon Green® and SNAP-cell 505-Star a 520/20 nm (BRET) filter was used to select the acceptor emission peaks. TagRFP, HaloTag® TMR-Direct and SNAP-cell TMR-Star emissions were detected with a 530 nm long pass filter. For HaloTag® NanoBRET 618 a 620/20 nm filter was used and a 600 nm long pass filter was applied for the BRET acceptors mCherry and SNAP-cell 647SiR. The integration time per data point was set to 0.3 s.

Experiments with higher temporal resolution were performed employing the Synergy Neo2 (BioTEK) plate reader, which is equipped with injectors and has a faster acquisition time. Data were acquired in well-mode, the acquisition interval was set to 1 s and the integration time to 0.3 s. After acquisition of baseline for 180 s, 10 µL of solution with or without ligand (buffer control) were injected with a speed of 225 µL s^{-1} (delivery time = 44 ms) and the signal was recorded for 180–360 s.

Receptor staining. Cells were co-transfected with FRET-based sensors to monitor downstream signaling and the wild type or the BRET-biosensor receptor as described above. Staining of the plasma membrane portion of the receptors was evaluated using a cell-impermeable anti HA-tag conjugated with AlexaFluor594 (Anti-HA-AlexaFluor594 ThermoFischer) or Anti-Flag® M2 conjugated with Cy3 (Anti-Flag® M2 Cy3, Sigma). The fluorescent antibodies were diluted in DMEM to a concentration of 10 µg mL^{-1} and incubated for 1 h at 37 °C in the 96-well plates. Subsequently, cells were rinsed three times and incubated additional 30 min with fresh DMEM.

Subsequently, the emission intensity of HEK-TSA cells were measured using the Synergy Neo2 plate reader. Therefore, cells stained with Anti-Flag® M2 Cy3 ($\beta_2AR_{NLuc/Halo}$ or β_2AR) were excited using a 540/20 nm excitation and the emission intensity was recorded using 590/35 nm emission filter. Fluorescence intensities of HEK-TSA cells stained with Anti-HA-AlexaFluor594 were measured using a 590/20 nm (excitation)–620/15 nm (emission) filter combination.

Expression levels of $G\alpha_{i2}$-FRET and H187-EPAC-FRET sensor. The Synergy Neo2 plate reader was employed to assess the expression levels of the downstream sensors ($G\alpha_{i2}$-FRET and H187-EPAC-FRET sensor). Therefore, the FRET

acceptors (cpVenus173 and tandem cpVenus173) were directly excited using a 500/20 nm excitation filter. Emission intensities were detected with a 540/20 nm filter.

Membrane preparations. Membranes expressing wild-type α_{2A}AR (α_{2A}AR-wt) were harvested from HEK-TSA cells grown in 15 cm dishes, 48 h after transfection. Membranes expressing the BRET-based α_{2A}AR sensor ($\alpha_{2A}AR_{Nluc/Halo}$) were obtained from HEK293 stably expressing the sensor. Cells were detached from the dishes with a cell scraper and suspended in Tris buffer (5 mM Tris, 2 mM EDTA, pH 7.4). After centrifugation for 10 min at 1000 × *g*, cells were re-suspended in buffer 1 (20 mM HEPES, 10 mM EDTA, PBS, pH 7.4) and homogenized using twice Ultraturax for 15 s. The suspension was centrifuged for 10 min at 3200 × *g*. The resulting supernatant was further centrifuged for 45 min at 37,000 × *g* and 4 °C. The pellet was resuspended and the last two centrifugation steps were repeated. The pellet was then suspended in binding buffer (50 mM Tris, 100 mM NaCl, 3 mM $MgCl_2$, pH 7.4) and the amount of total membrane protein was measured using the Pierce BCA Protein Assay Kit according to the manufacturer's instructions.

Radioligand binding. Total radioligand binding was assessed by incubating 5 µg of membrane protein with different concentrations (0.04–12 nM) of the antagonist α_{2A}AR radioligand [^{3}H]RX821002. To define unspecific binding, 20 µM phentolamine was added. Competition binding was performed by incubating 2 µg membrane protein with 0.3–2.0 nM [^{3}H]RX821002 and increasing concentrations of the different α_{2A}AR ligands in the presence (=low affinity state for agonists) and absence (=high-affinity state for agonists) of 10 µM GTP. Following incubation for 1 h at room temperature, membranes were transferred to Millipore glass-fiber filters via vacuum filtration. These filters were incubated with scintillation cocktail and membrane-bound radioactivity was measured with a scintillation counter.

Data analysis and statistics. FRET and BRET ratios before ($Ratio_{basal}$) and after ligand or buffer application ($Ratio_{stim}$) were defined as acceptor emission/donor emission and corrected for donor bleedthrough into the acceptor channel by subtracting the averaged ratio of the unlabeled control (UC). For cells expressing biosensors with a fluorescent protein as acceptor, the averaged UC ratio of the analogous HaloTag construct was considered for bleedthrough correction.

To quantify the ligand induced conformational change, ΔFRET or ΔBRET was calculated for each well as a percent over basal ((($Ratio_{stim} - Ratio_{basal}$)/$Ratio_{basal}$) × 100) and subtracted by the averaged ΔFRET or ΔBRET of buffer.

Z-factors expressing the high-throughput suitability were calculated with the following equation:

$$Z = 1 - \frac{(3\sigma_S + 3\sigma_C)}{(\mu_S - \mu_C)}$$

where σ_s and σ_c are the standard deviations of ΔFRET or ΔBRET. μ_S and μ_C express the mean of ΔFRET or ΔBRET values of positive and negative control, respectively. If the positive control induced a decrease in the energy transfer (negative ΔRET as for $\alpha_{2A}AR_{CFP/YFP}$, $\beta_2AR_{NanoLuc/Halo\mathbf{618}}$, $PTHR1_{NanoLuc/Halo\mathbf{618}}$, $PTHR1_{CFP/YFP}$) the denominator in equation is inverted ($\mu_C - \mu_S$). As a positive control, we defined epinephrine for the α_{2A}AR- and β_2AR-sensors and PTH(1-34) for PTHR1 sensors. Buffer was used as a negative control in all *Z* factor experiments.

For simplicity, all agonist-induced RET changes were consistently plotted as ascending curves or bars. Therefore, *y*-axes in all figures were inverted if agonists for the respective biosensor induced a reduction of the ratio.

Data were analyzed using Prism 5.0 software (GraphPad) and expressed as mean ± s.e.m. Data from concentration–response experiments were fitted using a mono-exponential curve four-parameter fit. Radioactivity values from binding experiments were analyzed using a one-site fitting model if GTP was added prior the experiment. Data from competition-binding experiments without exogenously added GTP were first analyzed for the statistically preferred fitting model applying extra-sum-of squares F-test comparing a one-component vs. two-component fit. Superiority of the two-component model was confirmed for all agonists (partial or full) tested. The two-component fit was then conducted with the fraction of the high-affinity component (R_H) fixed to 0.58 which is the mean R_H of all data where this model was applied. Statistical differences were evaluated using one-way ANOVA test followed by Bonferroni multiple comparison, Student's *t*-test or extra-sum-of squares F-test. Differences were considered significant for values of $p < 0.05$.

Data availability. The datasets generated during and/or analysed during the current study are available at the homepage of the Institute of Pharmacology and Toxicology http://www.pharmakologie.uni-wuerzburg.de/fileadmin/03250100/user_upload/Schihada_et_al._CommsBio_2018_-_Figure_1-3.zip

Received: 28 November 2017 Accepted: 11 May 2018
Published online: 07 August 2018

References

1. Rasmussen, S. G. et al. Crystal structure of the beta2 adrenergic receptor-Gs protein complex. *Nature* **477**, 549–555 (2011).
2. Granier, S. et al. Structure and conformational changes in the C-terminal domain of the beta2-adrenoceptor: insights from fluorescence resonance energy transfer studies. *J. Biol. Chem.* **282**, 13895–13905 (2007).
3. Dacres, H., Wang, J., Dumancic, M. M. & Trowell, S. C. Experimental determination of the Forster distance for two commonly used bioluminescent resonance energy transfer pairs. *Anal. Chem.* **82**, 432–435 (2010).
4. Vilardaga, J. P., Bunemann, M. & Krasel, C. et al. Measurement of the millisecond activation switch of G protein-coupled receptors in living cells. *Nat. Biotechnol.* **21**, 807–812 (2003).
5. Bünemann, M., Vilardaga, J. P., Hoffmann, C. & Lohse, M. J. Millisecond activation switch for seven-transmembrane proteins. United States Patent US20060272037 A1 (2002).
6. Hoffmann, C. et al. A FlAsH-based FRET approach to determine G protein-coupled receptor activation in living cells. *Nat. Methods* **2**, 171–176 (2005).
7. Stumpf, A. D. & Hoffmann, C. Optical probes based on G protein-coupled receptors-added work or added value? *Br. J. Pharmacol.* **173**, 255–266 (2016).
8. Lohse, M. J., Maiellaro, I. & Calebiro, D. Kinetics and mechanism of G protein-coupled receptor activation. *Curr. Opin. Cell Biol.* **27**, 87–93 (2014).
9. Patterson, G. H., Piston, D. W. & Barisas, B. G. Forster distances between green fluorescent protein pairs. *Anal. Biochem.* **284**, 438–440 (2000).
10. Szalai, B. et al. Allosteric interactions within the AT(1) angiotensin receptor homodimer: role of the conserved DRY motif. *Biochem. Pharmacol.* **84**, 477–485 (2012).
11. Dacres, H. et al. Greatly enhanced detection of a volatile ligand at femtomolar levels using bioluminescence resonance energy transfer (BRET). *Biosens. Bioelectron.* **29**, 119–124 (2011).
12. Sleno, R. et al. Designing BRET-based conformational biosensors for G protein-coupled receptors. *Methods* **92**, 11–18 (2016).
13. Devost, D. et al. Conformational profiling of the AT1 angiotensin II receptor reflects biased agonism, G protein coupling and cellular context. *J. Biol. Chem.* **292**, 5443–5456 (2017).
14. Hall, M. P. et al. Engineered luciferase reporter from a deep sea shrimp utilizing a novel imidazopyrazinone substrate. *ACS Chem. Biol.* **7**, 1848–1857 (2012).
15. Zhang, J. H., Chung, T. D. & Oldenburg, K. R. A simple statistical parameter for use in evaluation and validation of high throughput screening assays. *J. Biomol. Screen.* **4**, 67–73 (1999).
16. Keppler, A. et al. Labeling of fusion proteins of O6-alkylguanine-DNA alkyltransferase with small molecules in vivo and in vitro. *Methods* **32**, 437–444 (2004).
17. Los, G. V. et al. HaloTag: a novel protein labeling technology for cell imaging and protein analysis. *ACS Chem. Biol.* **3**, 373–382 (2008).
18. Machleidt, T. et al. NanoBRET-A Novel BRET platform for the analysis of protein-protein interactions. *ACS Chem. Biol.* **10**, 1797–1804 (2015).
19. De Lean, A., Stadel, J. M. & Lefkowitz, R. J. A ternary complex model explains the agonist-specific binding properties of the adenylate cyclase-coupled beta-adrenergic receptor. *J. Biol. Chem.* **255**, 7108–7117 (1980).
20. Lohse, M. J., Nuber, S. & Hoffmann, C. Fluorescence/bioluminescence resonance energy transfer techniques to study G-protein-coupled receptor activation and signaling. *Pharmacol. Rev.* **64**, 299–336 (2012).
21. van der Westhuizen, E. T., Breton, B., Christopoulos, A. & Bouvier, M. Quantification of ligand bias for clinically relevant beta2-adrenergic receptor ligands: implications for drug taxonomy. *Mol. Pharmacol.* **85**, 492–509 (2014).
22. Reiner, S., Ambrosio, M., Hoffmann, C. & Lohse, M. J. Differential signaling of the endogenous agonists at the beta2-adrenergic receptor. *J. Biol. Chem.* **285**, 36188–36198 (2010).
23. Liu, J. J., Horst, R. & Katritch, V. Biased signaling pathways in beta2-adrenergic receptor characterized by 19F-NMR. *Science* **335**, 1106–1110 (2012).
24. Sungkaworn, T. et al. Single-molecule imaging reveals receptor-G protein interactions at cell surface hot spots. *Nature* **550**, 543–547 (2017).
25. Braeuning, A. Firefly luciferase inhibition: a widely neglected problem. *Arch. Toxicol.* **89**, 141–142 (2015).
26. White, C. W., Vanyai, H. K. & See, H. B. Using nanoBRET and CRISPR/Cas9 to monitor proximity to a genome-edited protein in real-time. *Sci. Rep.* **7**, 3187 (2017).
27. van Unen, J. et al. A new generation of FRET sensors for robust measurement of Galphai1, Galphai2 and Galphai3 activation kinetics in single cells. *PLoS ONE* **11**, e0146789 (2016).
28. Maurel, D. et al. Cell-surface protein-protein interaction analysis with time-resolved FRET and snap-tag technologies: application to GPCR oligomerization. *Nat. Methods* **5**, 561–567 (2008).

29. Klarenbeek, J., Goedhart, J. & van Batenburg, A. Fourth-generation epac-based FRET sensors for cAMP feature exceptional brightness, photostability and dynamic range: characterization of dedicated sensors for FLIM, for ratiometry and with high affinity. *PLoS ONE* **10**, e0122513 (2015).

Acknowledgements

We thank Professor Karl-Norbert Klotz for the useful discussion and Kevin F. Webb for critically reading the manuscript. We thank Professor Joachim Goedhart (Section Molecular Cytology, University of Amsterdam, Amsterdam, The Netherlands) for providing the $G\alpha_{i2}$-FRET sensor, and Kees Jalink (The Netherlands Cancer Institute, Amsterdam, The Netherlands) for providing the H187-EPAC-FRET sensor. This work was supported by the Federal Ministry of Research (BMBF; 03V0830) to M.J.L.

Author contributions

M.J.L. and I.M. conceived the study. H.S. designed, performed, analyzed the experiments and interpreted the data. S.V. performed the experiments. H.S., M.F., and U.Z. cloned the constructs. I.M. designed, analyzed, and interpreted the data. I.M. and H.S. wrote the paper. M.J.L. designed and interpreted the data and edited the paper. All authors read, revised, and approved the manuscript.

Additional information

Supplementary information accompanies this paper at https://doi.org/10.1038/s42003-018-0072-0.

Competing interests: The authors declare that The University of Würzburg holds a patent on this technology: WO2004057333 A1.

Reprints and permission information is available online at http://npg.nature.com/reprintsandpermissions/

Publisher's note: Springer Nature remains neutral with regard to jurisdictional claims in published maps and institutional affiliations.